JMEPEG (2005) 14:322-326
DOI: 10.1361/10599490523940

1059-9495/$19.00

Effect of Joint Design on Mechanical Properties of AL7075 Weldment

Leijun Li, Kevin Orme, and Wenbin Yu

(Submitted December 2, 2004; in revised form March 21, 2005)

The effects of joint design on the mechanical properties of AL7075-T6 aluminum sheet were studied on the latest automated gas-tungsten arc-welding system. Using ER5356 filler metal, full-penetration welds were made on workpieces with various included joint angles. Testing of the mechanical properties of the joints was done in the as-welded, naturally aged, and postweld heat-treated conditions. The results show that by using crack-resistant filler, and by selecting the proper joint design and postweld heat treatment, strong, dependable welds can be produced on thin AL7075 sheet material. An elasticity model of the weld joint was established to help understand the mechanical behavior of the joints. An undermatched joint design is shown to be capable of achieving a joint strength that matches the strength of the base alloy.

Keywords AL7075, automated gas-tungsten arc welding, joint design, mechanical properties

1. Introduction

Aluminum 7075 is a high-strength, heat-treatable alloy that is commonly used in aerospace and automotive applications, or in areas in which specific strength is a concern. Frequently, the welding of AL7075 is required, but weldments made from AL7075 are typically much lower in strength, ductility, and corrosion resistance than the unaltered base metal (Ref 1, 2). The literature treats AL7075 as an unweldable alloy and advises against welding it. The cracking susceptibility in the heat-affected zone has been studied by Huang and Kou in a series of articles (Ref 3-6). The welding of AL7075 usually involves using a non-heat-treatable filler metal such as ER5356 to increase the hot-cracking resistance of the weld fusion zone. The strength of the joint, on the other hand, decreases due to the lower strength of the non-heat-treatable filler metal. The mixing of base metal AL7075 into the weld fusion zone, however, will increase the hardenability of the weld, and a higher-strength weld joint is possible. The amount of base metal mixed into the weld is a function of groove design and welding parameters. Even for an optimized weld joint and groove design, consistent control of hot-cracking sensitivity is difficult to achieve due to the variability of the welding parameters in practice.

Recent developments in computer-controlled automated welding systems makes it possible to consistently reproduce an optimized welding procedure. Such new technology increases the possibility of welding previously "unweldable" materials. This article reports on a study of automated gas-tungsten arc welding (GTAW) of AL7075-T6 to demonstrate how fusion zone composition can be consistently controlled by joint design and welding parameters. The effect of weld composition on the mechanical properties of welded joints was also examined.

Leijun Li, Kevin Orme, and **Wenbin Yu,** Department of Mechanical & Aerospace Engineering, Utah State University, Logan, UT 84322-4130. Contact e-mail: leijun.li@usu.edu.

2. Experimental Procedures

Commercial AL7075 sheet with a thickness of 3.175 mm (1/8 in.) and filler wire ER5356 with a diameter of 0.9 mm (0.035 in.) were selected for this study. Table 1 shows the nominal chemical composition of these two alloys.

Welding was conducted using a power supply that was capable of digitally controlling all welding parameters. A computer-controlled wire feeder was integrated with a gantry table to provide filler metal and welding torch motion. Preliminary experiments were conducted to select the welding parameters that gave the best bead shape, penetration, cleaning action, and cracking resistance. The following conditions were selected based on the preliminary experiments and were kept constant in this study:

- Alternating current frequency 400 Hz;
- Average current ratio of direct current electrode negative (DCEN) to direct current electrode positive (DCEP) of 3.56:1;
- Unbalanced current waveform with 68% DCEN to 32% DCEP;
- Shielding gas 70% argon and 30% helium;
- 3.175 mm diameter pure W electrode with a 3.175 mm diameter ball tip;
- Electrode workpiece distance equal to 2 mm; and
- Welding speed equal to 40.6 cm/min.

Five different groove designs were used in this study to obtain a full penetration and a consistent weld metal profile. As such, current levels and wire feed speed were adjusted for each groove design. Different base metal dilution ratios were simulated by changing the included angles of the V-groove butt joint design. The included angles of 0, 25, 50, 75, and 90° were prepared as shown in Fig. 1.

The test pieces were cleaned and clamped with bolts (tightened to 50 ft-lb) onto a fixture that provided the back purge for the weld root with argon. The welded samples were tested under three different conditions: (a) as-welded; (b) heat treatment to T6 temper; and (c) naturally aged for 30 days at room temperature. The T6 temper was accomplished by heating the sample to 460 °C (860 °F) for 10 min, quenching into water,

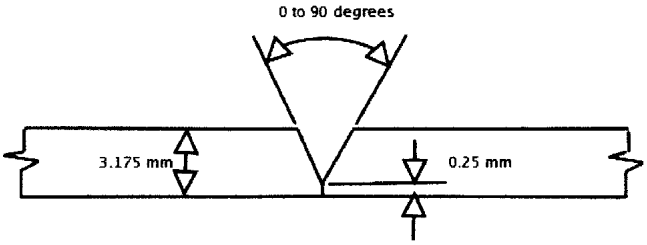

Fig. 1 The V-groove butt joint design

Table 1 Nominal chemical compositions of AL7075 and ER5356

Element	AL7075 nominal, wt.%	ER5356 nominal, wt.%
Si	0.40	0.50
Fe	0.50	…
Cu	1.2-2.0	0.10
Mn	0.30	0.50-0.20
Mg	2.1-2.9	4.5-5.5
Cr	0.18-0.28	0.05-0.20
Zn	5.1-6.1	0.10
Ti	0.20	0.06-0.20
Al	Balance	Balance

and then reheating to 121 °C (250 °F) for 24 h. Tensile tests were conducted on samples extracted across the weld bead. Rockwell B hardness measurements were also taken from various regions of the test samples.

Microstructural analysis was conducted on the welded joints. The fusion zone cross-sectional areas were measured using digital-imaging software. The chemical composition of the base metal, filler metal, and weld metals were determined by chemical analysis.

3. Results

With the above welding procedures, defect-free and uniform weld beads were obtained. The cross-sectional views of weld joints with different groove designs are shown in Fig. 2. A consistent weld bead shape was obtained for all groove designs.

The mechanical properties of the joints, as a function of joint design and postweld heat treatment, are shown in Fig. 3 and 4. In the as-welded condition, the yield strength of joints with various groove angles shows a variation from 200 to 230 MPa (Fig. 3). This indicates a weak effect due to joint design, and thus to variations in the chemical composition of the fusion zone, on the as-welded joint strength. Natural aging increases the yield strength of all joints to approximately 280 MPa, except for the joint with a 90° joint angle. This configuration did not show a significant increase in yield strength. The joint with 90° angle also contains the highest quantity of ER5356 (non-heat-treatable) filler metal. Dramatic changes in yield strength were obtained following a T6 heat treating. All joint angles showed a significant increase in the yield strength, with the greatest gain (to 486 MPa) occurring for the 0° angle joint. The smallest gain (to 259 MPa) occurred for the 90° angle joint. The AL7075 sheet used in this study had a 494 MPa yield strength.

The ductility of the joints is also affected by the joint design and heat treatment conditions. This is shown in Fig. 4. In the as-welded condition, all joints showed elongation-to-failure values of between 2.7 and 3.4%. Consequently, no significant variations in ductility were seen among the different joint designs when the joints were tested in the as-welded condition. Natural aging had the effect of decreasing the ductility of all joints to <2.8%, except for the joint with the 0° groove angle. No apparent changes in ductility were observed for the 0° groove angle joint following natural aging. The T6 heat treating produced more dramatic changes in ductility. The joint with 0° angle showed a significant increase in elongation to 5.1%. The T6 heat treatment did not significantly change the elongation of the 25° and 50° joint angles with respect to the as-welded values. Significant decreases in ductility were observed in the joints with the 75° and 90° joint angles following the T6 heat treatment. The 90° angle joint showed an elongation decrease to 0.9%. The highest ductility among the joints (5.1%) is still about one-third that of the AL7075 sheet used in this study (14.8% elongation).

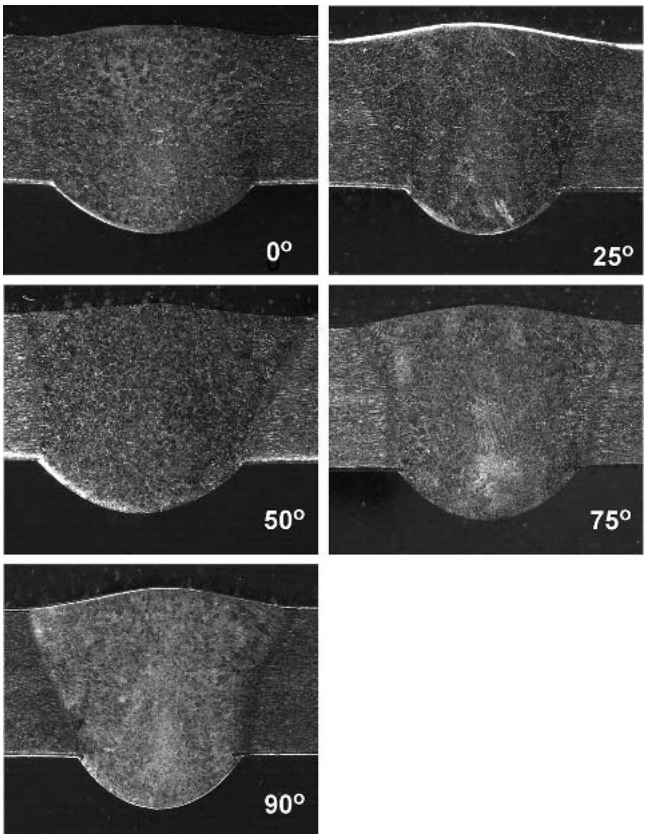

Fig. 2 Macroscopic photos of a cross-sectional view of the weld bead made with different groove angles

For a given base and filler metal, the chemical composition of the weld fusion zone is determined by the ratio of mixing during fusion. The fusion zone cross-sectional area for each joint design was measured, and the results are shown in Fig. 5. Based on the area information and groove design, the ratio of mixing of ER5356 filler metal and AL7075 base metal was calculated for each joint. A chemical analysis of ER5356 and AL7075 was conducted (Table 2), and the fusion zone composition of each joint design was precisely determined, owing to the automated nature of the GTAW process, which gave uniform and reproducible weld bead shapes and dimensions.

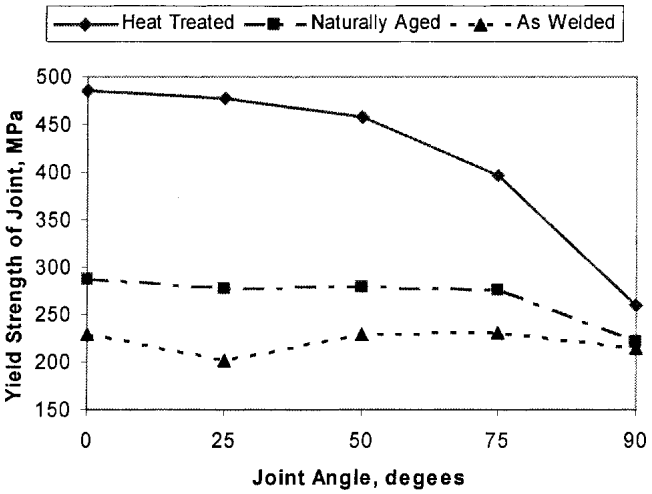

Fig. 3 Yield strength of the joints as affected by the joint angle and postweld heat-treating conditions

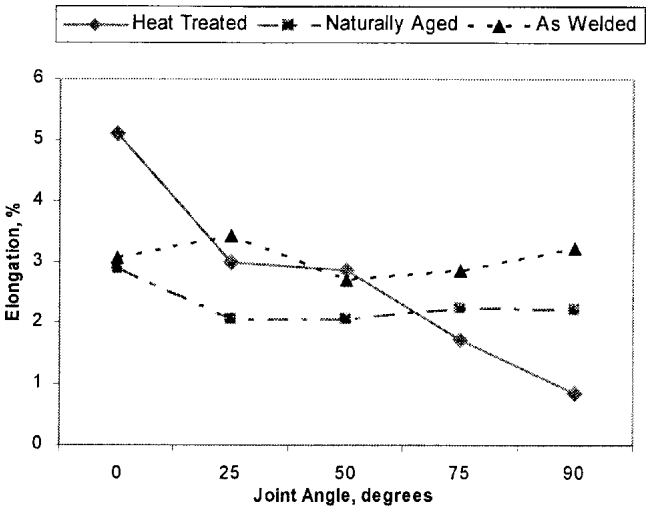

Fig. 4 Ductility of the joints as a function of joint angle and postweld heat-treating conditions

Table 2 Measured chemical composition of AL7075 and ER5356

Element	AL7075, wt.%	ER5356, wt.%
Si	0.08	0.16
Fe	0.2	0.42
Cu	1.5	0.05
Mn	0.05	0.05
Mg	2.49	4.28
Cr	0.19	0.05
Zn	5.76	0.04
Ti	0.04	0.08
Al	Balance	Balance

Figure 6 summarizes the concentration changes in Zn, Mg, and Cu in the weld fusion zones as a function of groove angles. The composition of the 0° angle weld is close to that of the AL7075 sheet, and the composition of the 90° angle weld is close to that of ER5356 filler metal.

The strengthening effect, particularly the precipitation strengthening associated with heat treating, is mainly affected

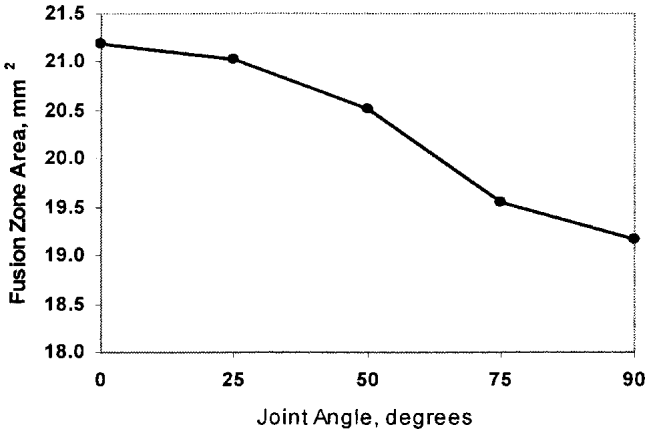

Fig. 5 Fusion zone cross-sectional area as a function of joint angle

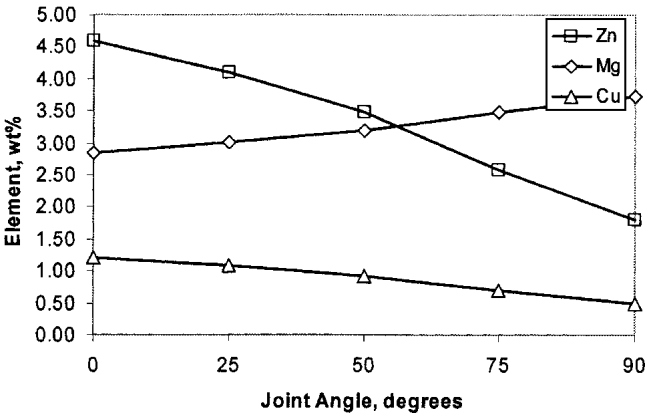

Fig. 6 The chemical composition of the weld fusion zone as a function of joint angle

by Zn, Cu, and Mg in the alloy. A comparison between the post-weld heat treatment (PWHT) microstructures of the 0° angle and 90° angle weld fusion zones was made (Fig. 7, 8). For the 0° angle, the weld fusion zone (Fig. 7) contains a greater number of precipitates following the T6 heat treatment. The 90° angle weld fusion zone contained far fewer precipitates following the heat treatment (Fig. 8).

4. Discussion

The mechanical properties of the joints measured in this study were from transverse sections with the weld metal groove perpendicular to the tensile loading direction. The properties measured were composed of contributions from a composite of the base metal, heat-affected zone, and fusion zone. To shed some light on the contribution of each individual zone to the overall properties of the entire joint, and to analyze the effect of the groove design on joint properties, an idealized joint was analyzed using linear elasticity theory.

As shown in Fig. 9, the width of the welded specimen is 25.4 mm along x_3, the height is 3.175 mm along x_2, and the length is 304 mm. Due to symmetry, only half of the specimen was needed for the analysis, which means L equals 152 mm. The weld zone was idealized as a trapezoid with the inclined edge making an angle of α with respect to x_3. The heat-affected zone was considered as part of the base metal. The values for

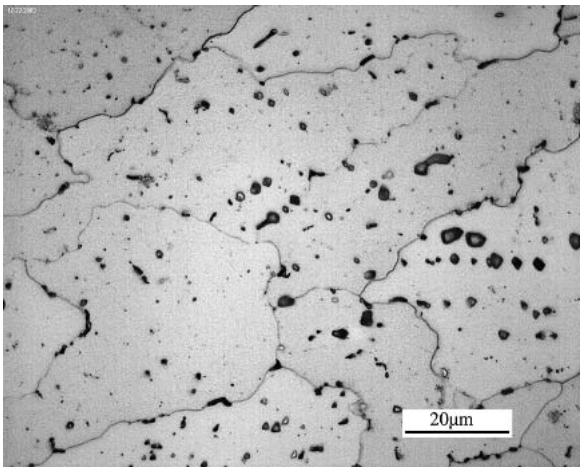

Fig. 7 Microstructure of the 0° angle weld fusion zone after the T6 heat treatment (880×)

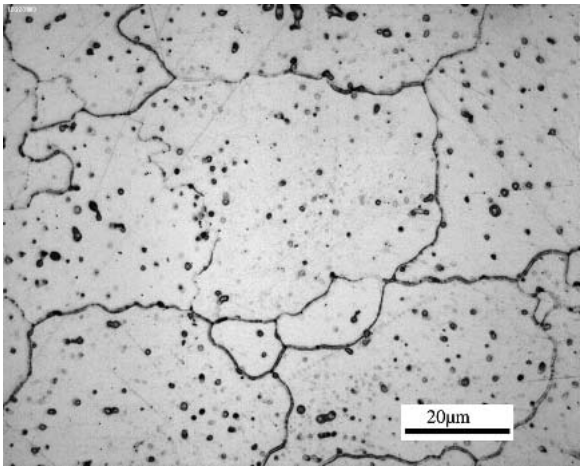

Fig. 8 Microstructure of the 90° angle weld fusion zone after the T6 heat treatment (880×)

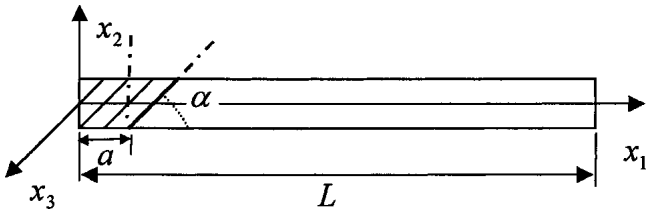

Fig. 9 The model for the elastic stress analysis

the half-weld root width (a) and the inclined angle (α) can be measured from the welded joints. According to the test condition, the end faces along x_3 are free to move, which means that the problem is one of plane stress within the x_1 x_2 plane. Letting $u(x_1,x_2)$ and $v(x_1,x_2)$ denote the in-plane displacements, the governing equations can be written as:

$$\frac{E}{1-\upsilon^2}\left(\frac{\partial^2 u}{\partial {x_1}^2}+\frac{1-\upsilon}{2}\frac{\partial^2 u}{\partial {x_2}^2}+\frac{1+\upsilon}{2}\frac{\partial^2 v}{\partial x_1 \partial x_2}\right)=0$$

$$\frac{E}{1-\upsilon^2}\left(\frac{\partial^2 v}{\partial {x_2}^2}+\frac{1-\upsilon}{2}\frac{\partial^2 v}{\partial {x_1}^2}+\frac{1+\upsilon}{2}\frac{\partial^2 u}{\partial x_1 \partial x_2}\right)=0$$

where E is Young's modulus and υ is Poisson's ratio.

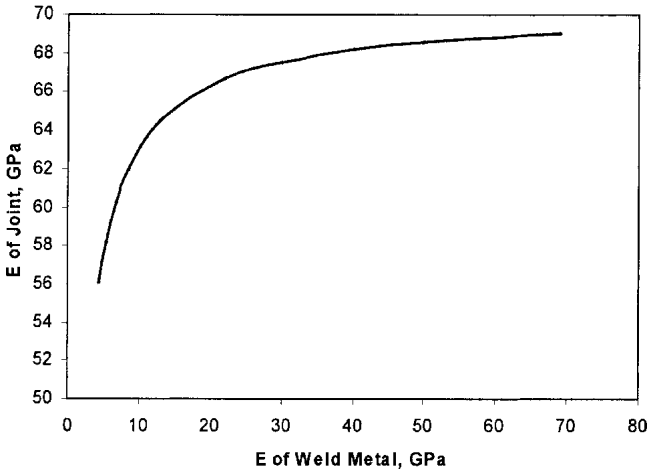

Fig. 10 The calculated results showing the relationship between E_w and E_j for a weld shape of $\alpha = 60°$ and $a = 2.0$ mm

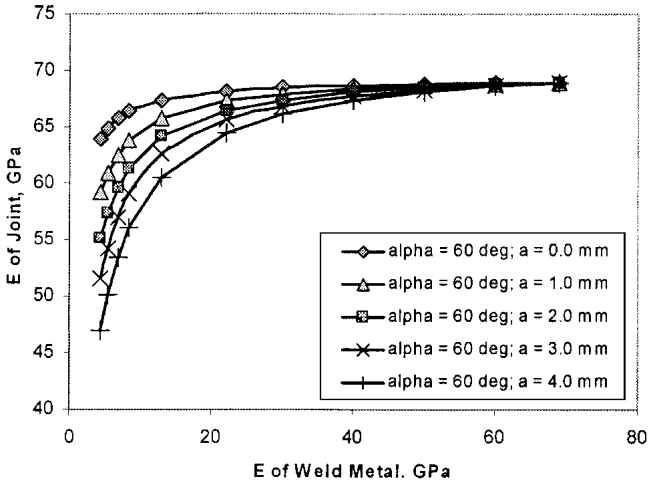

Fig. 11 Effect of a on the relationship between E_w and E_j

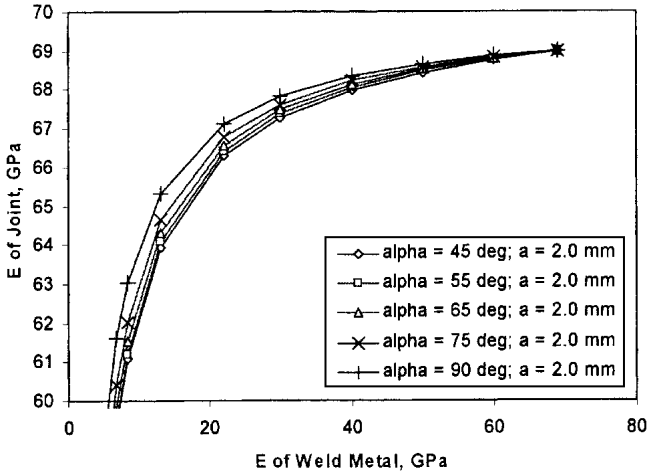

Fig. 12 Effect of α on the relationship between E_w and E_j

Due to symmetry considerations, the boundary conditions at the end of the specimen, $x_1 = 0$, are:

$$u(0,x_2)=0;\ v(0,0)=0$$

The boundary conditions at $x_1 = L$ are:

$$\int_{-h/2}^{h/2} \sigma_{11}(L,x_2)dx_2 = P; \int_{-h/2}^{h/2} \sigma_{12}(L,x_2)dx_2 = 0$$

where P is the applied force during testing, and σ_{11} and σ_{12} are the tensile stress and in-plane shear stress, respectively. Because the specimen was composed of two different regions, it is very difficult to solve this problem exactly. Instead, if the principle of minimum total potential energy is used along with the Ritz method (Ref 7), an approximate solution can be obtained, which is sufficient in this case. By assuming $u(x_1,x_2)$ and $v(x_1,x_2)$ to be polynomials in terms of x_1 and x_2, a set of algebraic equations can be solved in place of the original partial differential equations. A closed-form relationship between the overall value of E for the joint and those of individual zones as a function of a and α of the weld fusion zone was obtained.

The weld fusion zone shapes, as determined in this study (Fig. 2), can be approximated by a common dimension, $\alpha = 60°$ and $a = 2.0$ mm. For this common weld shape, the relationship between the Young's modulus of the weld metal (E_w) and the Young's modulus of the joint (E_j) is shown in Fig. 10. Clearly, E_j is a sensitive function of E_w for the given weld shape. It is noticeable that weak weld metal (i.e., with a low E_w) can achieve a significant joint strength (i.e., a high E_j). The 0° angle weld design had a fusion zone chemistry that gave the highest strength, which, according to this curve, was able to produce the strongest weld joint.

For a 60° angle, a is plotted for E_w and E_j. The results are shown in Fig. 11. Clearly, a narrower weld (i.e., smaller a values) gives a stronger joint, all other factors remaining constant. For an a value of 2.0 mm, the α is plotted for E_w and E_j. The results are shown in Fig. 12. As α increases, the weld fusion zone becomes narrower. Therefore, joint strength will increase. Apparently, this analysis is valid only for cases in which the deformation is elastic. If the entire stress-strain curve of the joint is examined, a numerical elastic-plastic analysis must be used, because a closed-form solution is not available.

5. Conclusions

Using the automated GTAW procedure, crack-free joints in the AL7075 sheet have been achieved. The joint strength approached that of the AL7075 sheet when ER5356 filler was used with a 0° groove angle and T6 postweld heat treatment. The ductility of the joint, however, was only one-third that of the unwelded base metal. The naturally aged joint samples increased in strength but decreased in ductility compared with the as-welded samples. The joint design has a significant effect on joint strength. A simplified elastic model can correctly predict the elastic mechanical behavior of the joint for different joint designs.

References

1. F.R. Collins, Improved Strengths in Welded High-Strength, Heat-Treatable Aluminum Alloys, *Welding J.,* Vol 41 (No. 8), 1962, p 337s-245s
2. J.H. Dudas and F.R. Collins, Preventing Weld Cracks in High-Strength Aluminum Alloys, *Welding J.,* Vol 45 (No. 6), 1966, p 241s-249s
3. C. Huang and S. Kou, Liquation Mechanisms in Multi-Component Aluminum Alloys During Welding, *Welding J.,* Vol 81 (No. 10), 2002, p 211s-222s
4. C. Huang and S. Kou, Partially Melted Zone in Aluminum Welds: Liquation Mechanism and Directional Solidification, *Welding J.,* Vol 79 (No. 5), 2000, p 113s-120s
5. C. Huang and S. Kou, Partially Melted Zone in Aluminum Welds: Solute Segregation and Mechanical Behavior, *Welding J.,* Vol 80 (No. 1), 2001, p 9s-17s
6. C. Huang and S. Kou, Partially Melted Zone in Aluminum Welds: Planar and Cellular Solidification, *Welding J.,* Vol 80 (No. 2), 2001, p 46s-53s
7. J.N. Reddy, *Energy and Variational Methods in Applied Mechanics,* John Wiley & Sons, Inc., New York, 1984